

*Review article***Initial bonding of ferric ion (Fe^{3+}) and amyloid beta ($\text{A}\beta$) peptide as the precondition for oxidative stress in Alzheimer's disease**Nikola Barić¹⁾, Mario Cetina²⁾

1) Presika 153, 52220 Labin, Istra, Croatia

2) University of Zagreb, Faculty of Textile Technology, Department of Applied Chemistry, Zagreb, Croatia

Abstract

Objective: The process of binding ferric ion Fe^{3+} to amyloid beta peptide ($\text{A}\beta$ peptide) is the prerequisite for its reduction into the redox active ferrous ion Fe^{2+} and its inclusion in the Fenton reaction with the creation of extremely toxic, aggressive hydroxyl radical $\cdot\text{OH}$, the fundamental key in the pathology and pathophysiology of Alzheimer's disease (AD). The clearly defined cause and effective therapy for this fatal chronic neurodegenerative disease, unfortunately, has still not been discovered. Related to old age and ageing, and due to AD's continuing absolute and relative increase in the elderly population, particularly in the developed world countries, with its severity and the enormous costs of its prevention and treatment, this disease has become a significant burden on modern-day society. The binding of Fe^{3+} to $\text{A}\beta$ initiates a series of biochemical intermolecular activities that include electrostatic attraction of molecules, the formation of the complex metal ion of the octahedral structure and the creation of atomic hybrid orbitals. All these processes have been dealt with in this study; however, it is necessary to carry out further intensive investigations.

Methods: Through a detailed analysis of available studies by prominent researchers who investigate the causes of AD, studies that are particularly related to the problem of Fe^{3+} and $\text{A}\beta$ interaction, and by reviewing relevant literature from the field of molecular biology and organic and inorganic chemistry, and especially by consulting respected chemistry engineers, we have tried to provide the answers to some fundamental issues related to the mentioned interaction.

Results: The results of our analysis undoubtedly indicate the great importance of the His13-His14 sequence in the process of Fe^{3+} binding to $\text{A}\beta$. The octahedral structure of the metal complex with Fe^{3+} in the center indicates that there are two His13-His14 sequences, each containing three ligands (N, N, O) that are coordinated to the central atom. One sequence belongs to the incoming $\text{A}\beta$ monomer ($\text{A}\beta 1$) and the other belongs to the monomer on top of the already formed protofilament ($\text{A}\beta 2$).

Discussion: The detailed discussion shows results of investigations conducted by a number of prominent experts. Their findings to a great extent coincide with our opinion. Most of the researchers support the idea of the great importance of the His13-His14 sequence for the binding of Fe^{3+} , as well as the role of oxidative stress in AD pathology.

Conclusion: AD is increasingly becoming one of the main subjects of interest in contemporary medicine. The binding of Fe^{3+} to $\text{A}\beta$ is one of the most important issues that modern science tries to resolve. The increasing investment of great funds in these investigations and adequate efforts by research workers will surely provide adequate results in the near future.

KEY WORDS: Alzheimer's disease, His13-His14 amyloid β ($\text{A}\beta$) sequence, $\text{Fe}^{3+}/\text{A}\beta$ interaction, chelation therapy

Introduction

The increased number of recent investigations point out the crucial role of oxidative stress in the development and course of Alzheimer's disease (AD)¹⁻⁵. Hydroxyl radical ($\cdot\text{OH}$), as one of the central figures in these events, is the object of composed, multiprofile examinations. $\cdot\text{OH}$, which is the neutral form of the hydroxyl ion (^-OH), presents one of the strongest oxidative compounds, capable of intensive reactions with the surrounding biological structures^{4,5}. What

is oxidative stress? It essentially represents the imbalance between the great quantum of oxidative factors and the decreased possibility of the protective anti-oxidative body systems⁴⁻⁸. $\cdot\text{OH}$ generation is the consequence of the non-toxic, redox-inactive ferric ion (Fe^{3+}) reduction (electron gain) into a toxic, redox-active ferrous ion (Fe^{2+}), and its consequent oxidation by hydrogen peroxide (H_2O_2) through the Fenton reaction^{2,3,5}. Reduction develops by mediation

Contact address: Nikola Barić MD, PhD
Presika 153, 52220 Labin, Istra, Croatia
TEL: 385/052/852-008/ Email: nikola.baric@pu.t-com.hr
Co-author: Mario Cetina, Assoc Prof, PhD
University of Zagreb, Faculty of Textile Technology, Department of Applied Chemistry
Prilaz baruna Filipovića 28a, HR-10000 Zagreb, Croatia
TEL: 385-1-3712-590/ E-mail: mario.cetina@ttf.hr

of one residue (MetS35) on the beta two ($\beta 2$) chain of amyloid beta ($A\beta$) complex peptide, generated by the proteolysis of APP (amyloid precursor protein), which is the integral component of the neuronal membrane (*Fig. 1*)⁹⁻¹⁵.

A number of previous examinations pointed out the presence of the great iron ions agglomeration in the specific brain regions in AD patients (parietal and motor cortex, hippocampus, amygdala). This phenomenon was especially observed in the amyloid plaque regions. These facts pose the question about the way and the exact place of iron accumulation. The aim of this study is to try to give some answers about these problems^{2,3,10,13,16}.

AD is a serious, chronic and fatal neurodegenerative disease with yet fairly unknown polygenetic etiology. Its two forms, the early form (EOAD, early onset AD, 5% of all cases) which develops before the age of 65, and the late form (LOAD, late onset AD, 95% of all cases) which develops after the age of 65, provide practically the same clinical picture, accompanied by the fluctuating progressive course and fatal termination at the end^{5,17}.

The mutations of gene complexes: *APP* (β -amyloid precursor protein gene, 21q21.3); *PSEN1* (presenilin-1 protein coding gene, 14q24.2); *PSEN2* (presenilin-2 protein coding gene, 1q42.13), and *BACE1* (β secretase-1 protein coding gene, 11q23.3) lead to EOAD, and mutations of *APOE4* (apolipoprotein E coding gene, 19q13.32) and *ADAM10* (ADAM metalloproteinase Domain 10 protein coding gene-regulator of α -secretase activity-gene, 15q21.3) lead to LOAD^{5,17}.

The crucial characteristic of AD is the progressive development of dementia, which is practically unperceivable at the beginning, but later develops a gradually increasing dramatic course. Examinations indicate that the disease is marked with the phenomenon of two characteristic markers in brain tissues, β -amyloid plaques in the extracellular (neuropil), mostly perisinaptic space, and neurofibrillary tangles (NFT) in the neurons^{4,9,17}.

Without entering the AD clinical picture, this study has the aim to give a detailed analysis of the Fe^{3+} reduction into Fe^{2+} , i.e. the process of initial binding of Fe^{3+} with $A\beta$ peptide. The Fe^{3+} ions, which after the Fe^{2+} oxidation (in the interstitium, neuropil) into Fe^{3+} through astrocytes APP and CP (ceruloplasmin) activity are by great part fixed to the present $A\beta$, reduced in Fe^{2+} , and after the entrance into the Fenton reaction, give the aggressive $\cdot OH$. Where and how is Fe^{3+} bound with $A\beta$ and reduced into toxic redox-active Fe^{2+} ? Oshiro S and Hare D^{18,19} give an excellent presentation of the iron metabolism in the brain, especially the transport of Fe^{3+} ions from the blood stream (where they enter by the intestinal absorption from food) through the endothelial luminal membrane into the endosome (the crucial role of the transferrin [Tf] and its endothelial receptor, TfR1), the reduction of Fe^{3+} into Fe^{2+} by endosome reductase (ferric reductase), and transfer of Fe^{2+} by ferroportin1 (FPN1) into neuropil and its arrival to the astrocytes APP and CP^{18,19}.

A number of investigations point out that the binding site of Fe^{3+} with the $A\beta$ peptide (metal binding domain, MBD) encompasses the region of the $\beta 1$ strand with the included His6 (His = histidine), His13, and His14 residues. Analyses indicate that the immediate binding place is located on the imidazole ring nitrogen (N) on the histidine side chain^{11,13,15}.

Discussion

It is emphasized in the introduction that the crucial pathophysiological event in AD is oxidative stress. Its characteristic is the imbalance between the prevalence of the production and harmful effects of oxidative compounds (oxidants, oxidizers, oxidizing agents) in relation to the protective body mechanisms that counteract their action (primarily protective enzymes: catalase [CAT], glutathione peroxidase [GPx-1] – one of the most abundant members of the GPx family of enzymes, superoxide dismutase1 [SOD1]). In case of the weaker expression of the first two enzymes (CAT, GPx-1), the destruction of H_2O_2 in neutral water (H_2O) is decreased, and as the result its elevated quantity enters the Fenton reaction with consequent rise in toxic $\cdot OH$ production. The final result is the rise of extremely harmful lipid peroxidation, especially in neuronal membranes. A number of recent investigations also indicate the declined SOD1 activity in AD patients, especially in their temporal cortex. The SOD1, by donating two H atoms to the toxic $O^{\cdot -}$ (superoxide radical anion), changes it into the not so toxic H_2O_2 and molecular O_2 . The elevated $O^{\cdot -}$ concentration in the tissues strongly supports the oxidative stress. The declined CAT activity is induced through its elevated interaction with a high quantity of amyloid beta monomers in AD tissues. On the other hand, the decline in GPx-1 activity in AD is induced through AD-dependent reduction of hippocampal and frontal cortices levels of brain glutathione (GSH)^{4-8,15}.

It is emphasized that the generation of $\cdot OH$ is related to the oxido/reductive processes which are located on the $A\beta$ chains. MetS35, otherwise a strong reducer (electron donor), located on the $\beta 2$ strand of the incoming $A\beta 1$ monomer, approaches the $A\beta 2$ fixed monomer (the top of the protofilament) primarily in an oblique, non congruent manner. The close contact between two monomers is supported by the forming of AGE compound MOLD (methylglyoxal lysine dimer). The decline of the critical interspace border below 19 Å enables the electron "hop" from the S in MetS35 on the Fe^{3+} on MBD of $A\beta 2$ monomer. The Fe^{3+} reduction occurs accompanied with MetS35 oxidation with its transformation into a very aggressive MetS35 \cdot^+ (methionine sulfide radical). The produced Fe^{2+} enters into the Fenton reaction with the formation of toxic $\cdot OH$. With the activity of $O_2^{\cdot -}$ (especially active in oxidative stress), MetS35 \cdot^+ is oxidised into methionine sulfoxide (MetSO) which by the action of MsrA (methionine sulfide reductase type A) is reduced in the primary MetSO (*Fig. 1*)^{5,15,18,20,21}.

By using X-ray microspectroscopy, X-ray absorption spectroscopy, electron microscopy, and spectrophotometric synthetic iron (III) quantification techniques, Everett J *et al.*^{2,3} examined the interaction between $A\beta(1-42)$ and synthetic iron (III). They demonstrate the strong iron (III) accumulation in amyloid aggregates with their subsequent reduction ($A\beta$ activity) into the redox active iron (II) phase. The reduction was elevated by the presence of Al (aluminum). These experiments gave the explanation for the previously explored iron accumulation in amyloid plaques of AD brains.

Based on NMR studies, Nair NG *et al.*²², have demonstrated that histidine residues are the crucial complex site of transition metals on the $A\beta$. In the case of physiological pH (pH 7.4), histidine strongly binds Zn (II), Cu(II), and Fe(III) ions. Redox active Cu(II) and Fe(III)

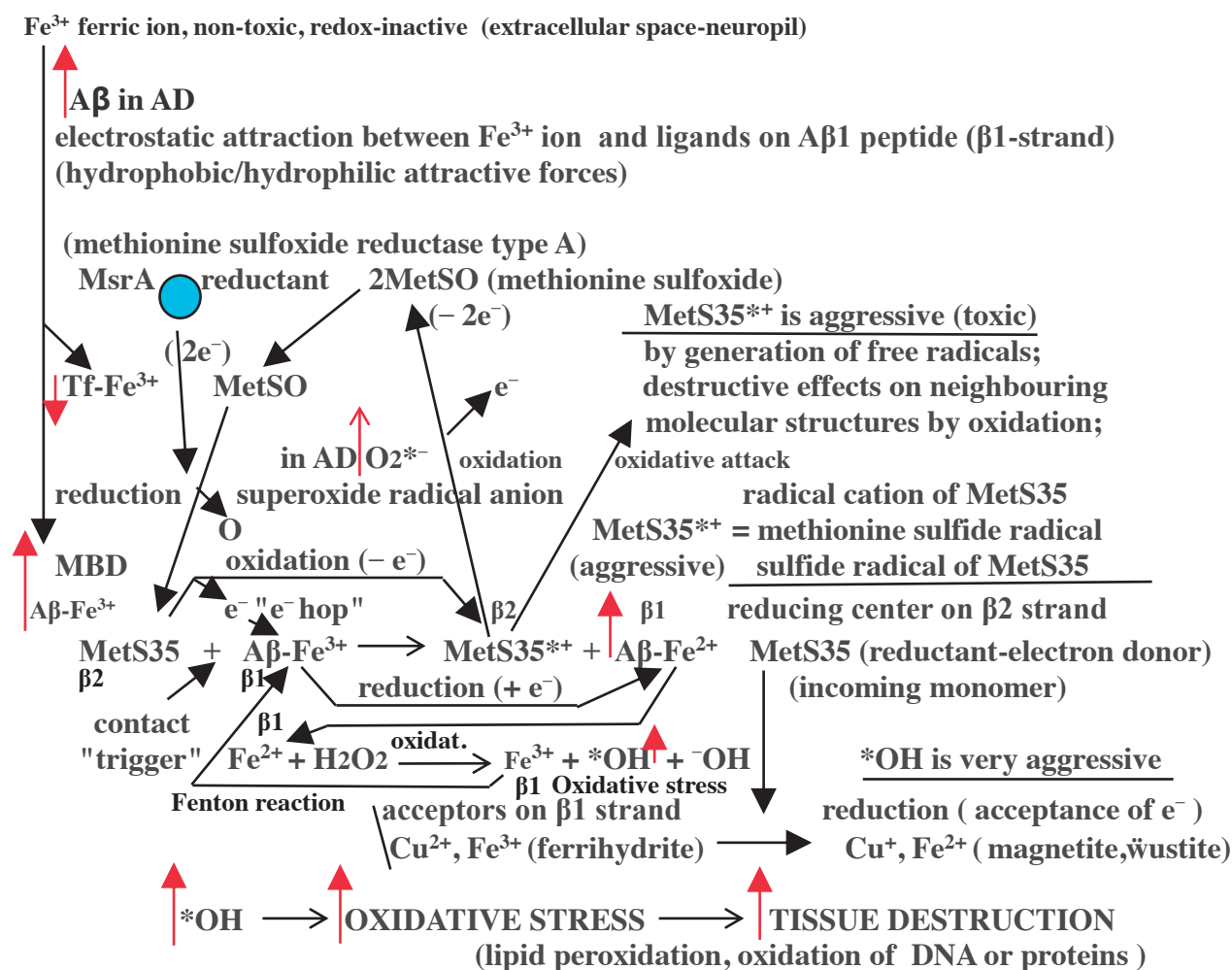


Fig. 1. Two ways for Aβ-mediated generation of destructive compounds.

Two ways: a) formation of very aggressive methionine sulfide radical and b) formation of *OH, destructive hydroxyl radical; oxidative stress, imbalance between elevated values of dangerous oxidants and weakened protective anti-oxidative body mechanisms; oxidation, electron loss; reduction, electron gain; MBD, metal binding domain, His13-His14 sequence on the N-terminal (β1-strand) of Aβ monomer; H_2O_2 , hydrogen peroxide, elevated values in oxidative stress; Cu, copper; Fe, iron; O, oxygen; S, sulphur.

Metal ion reduction is possible, not before the distance between MetS35, and their location drops below 19 Å; outer-sphere electron transfer; "electron hop," β1, Aβ- Fe^{3+} and β1, Aβ- Fe^{2+} represent the metal binding domain on β1-strand.

Aβ, amyloid beta; AD, Alzheimer's disease; His, histidine; Met, methionine; MetS35*•, methionine sulfide radical; MetSO, methionine sulfoxide; MsrA, MetSO reductase type A; Tf, transferrin; TfR1, transferrin receptor 1. Tf and TfR1 expression are reduced in AD.

ions are bound to histidine markedly more strongly than Zn (II). The strongest coordination site are imidazole nitrogen (N) atoms. The authors conclude that these metals have a crucial role in oxidative stress generation. They consider that the space organisation of ligands around the central metal atom is of octahedral structure. **Fig. 1** in the presented study visibly shows the two imidazole rings on the two oppositely positioned histidine molecules. Six ligands, 4 N atoms and 2 O atoms are clearly visible. Oxygen (O) sets off from C1 of the carboxyl group, and two N atoms are a part of NH_2 groups. 2 N, as was previously mentioned, are part of imidazole rings (**Fig. 2, 3**).

Streltsov *et al.* ¹⁴⁾, like Nair NG *et al.* ²²⁾, in their study

conclude that around the central metal ion there exists an octahedral space arrangement of ligands. Their experiments were carried out with Cu^{2+} ions. The space arrangement is determined by the combination of X-ray absorption spectroscopy (XAS) and density functional theory analysis of Aβ peptides complexed with Cu^{2+} . They conclude that the ligands are the following: N atoms from three histidine residues (His6, His13, His14, imidazole rings), carboxylate oxygen from either Glu11 (Glu = glutamine) or Asp1 (Asp = aspartic acid), and axial ligands formed from the water molecule (H_2O) and the second carboxyl O from Glu11 or Asp1.

Minicozzi V *et al.* ²³⁾ by a combination of complementary

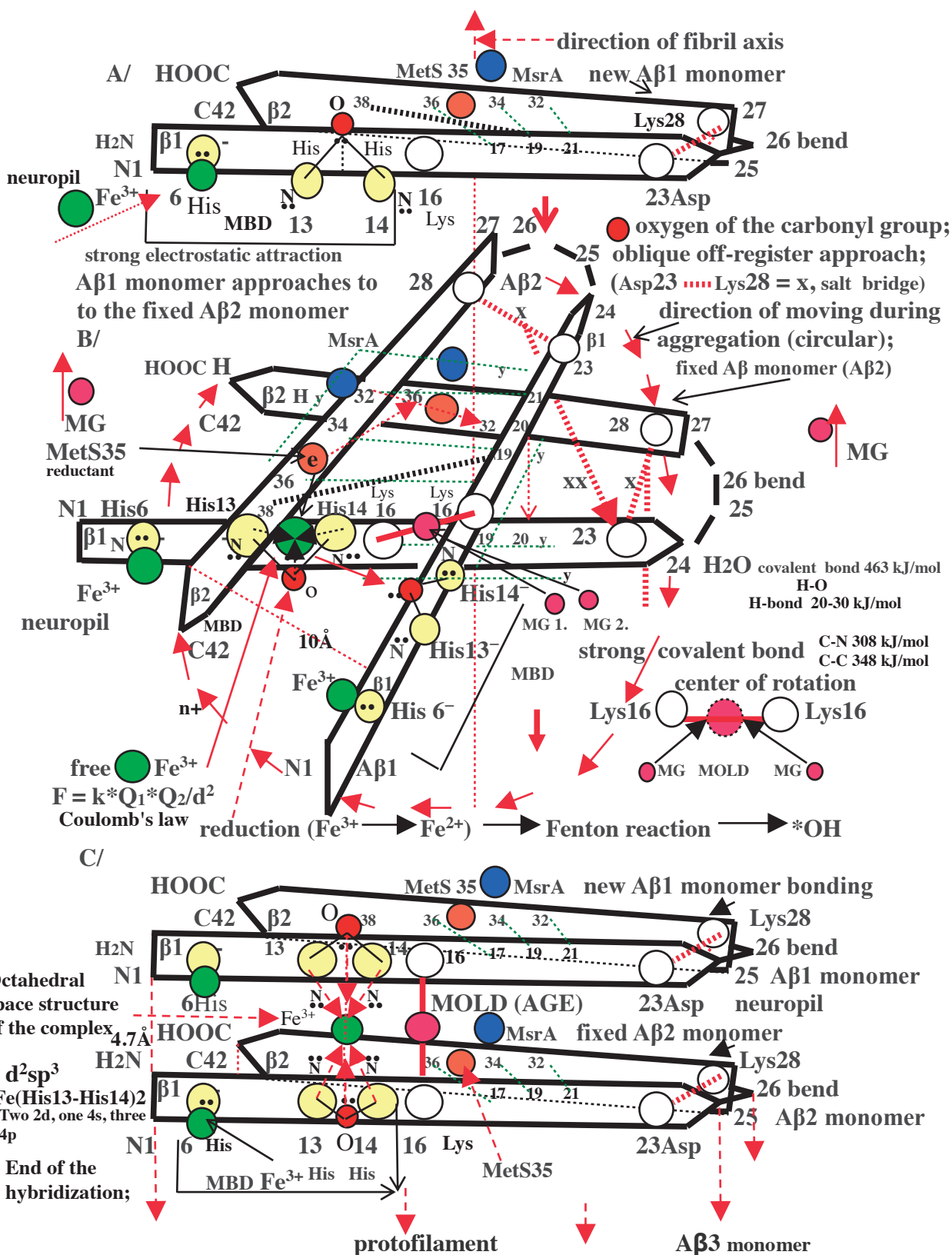


Fig. 2. Schematic presentation of the complex Fe (His13 - His14)₂ ion formation.

Section A/ : Presentation of the isolated A β -monomer before its contact with the fixed monomer on the tip of the protofilament; it is actually the electrostatic attraction between Fe³⁺ and His residues. **Section B/** : Oblique, nonparallel approach of A β 1 monomer and its clockwise rotation; onset of the Fe³⁺ reduction; MOLD formation. **Section C/** : Above four N and two O atoms are visible two dots (**) they represent electron lone pairs. MOLD, methylglyoxal lysine dimer, AGE compound; A β , amyloid beta; MBD, metal binding domain; His, histidine; Asp, aspartic acid; Lys, lysine; Met, methionine; MetS, methionine sulfide; MsrA, methionine sulfoxide reductase type A; MG, methylglyoxal; AGE, advanced glycation end product.

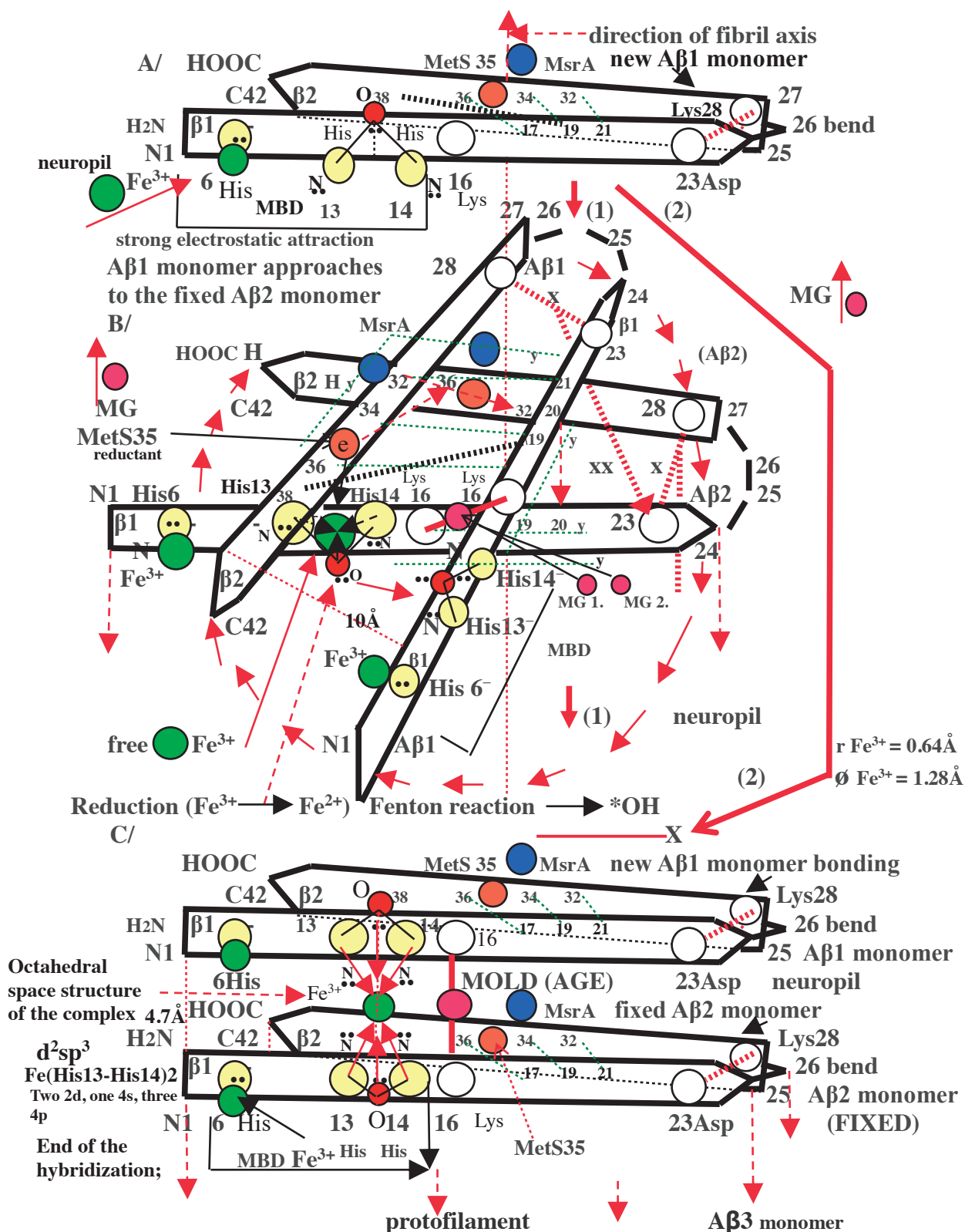


Fig. 3. Schematic presentation of the protofilament formation – aggregation process.

The new $\text{A}\beta$ monomer attracted by electrostatic, hydrophilic, and hydrophobic forces as well as H-bonds, arrives to the new protofilament top and will be fixed. Into its MBD enters the new free Fe^{3+} ion – **Section B/** on the figure. By the oblique, nonparallel approach the new $\text{A}\beta$ arrives, and the presented situation repeats: the contact between MetS35 and MBD (Fe^{3+}), reduction, rotation, and new ion complex formation; protofilament grows, aggregation proceeds; r , radius; $\text{A}\beta$, amyloid beta; MBD, metal binding domain; His, histidine; Asp, aspartic acid; Lys, lysine; Met, methionine; MetS, methionine sulfide; MsrA, methionine sulfoxide reductase type A; MG, methylglyoxal; AGE, advanced glycation end product.

experimental techniques, Sedimentation assay, Fourier Transform Infrared Spectroscopy, and X-ray Absorption Spectroscopy, determine the MBD structure in samples where A β is bound with Cu(II) or Zn(II). The Cu²⁺ binding is related to the imidazole group of histidine residues His6, His13, and His14 (the authors consider that this involves the peptide folding around the Cu²⁺ ion), and in Zn²⁺ binding, one histidine residue more is included. Both places were located in the N-terminal region of the β 1 amyloid beta peptide strand. It is very important to emphasize that in the case of Zn²⁺ are included four histidine residues (4N), two from each of the neighbouring parallel, congruently placed A β monomers. The presented model is very similar to our model (Fig. 1, 2).

Hane F and Leonenko Z²⁴) in their study about the metal effects on the A β aggregation kinetics, present the Cu²⁺ ions interaction through His13 and His14 on one A β monomer and His6 on the other. Both monomers are in the folding state.

Hedge ML *et al.*²⁵) in their study emphasize the abnormal metal ion accumulation in the brain during ageing and a number of neurodegenerative diseases, including AD. They especially emphasize the interplay between metal-protein and oxidative stress. Based on their experiments, they found a great A β accumulation connected with strong oxidative stress and metal-A β interaction. For AD pathology, the most important thing is the accumulation of copper, iron, and zinc.

Istrata AN *et al.*²⁶) emphasize that the A β 10-16 region is especially effective in metal attraction. His6, His13, and His14 are especially favourable for zinc binding. In the physiological conditions where Zn²⁺ is present, MBD forms homo et hetero-dimer complexes. It is clearly evident that Zn²⁺ influences the A β aggregation process. The mentioned residues are included in the electrostatic contact formation which can stabilize the intra and intermolecular interactions.

In what way does Fe³⁺ arrive on the MBD of A β 2 β 1 chain and where is the exact position of binding? It is said in the introduction that Fe³⁺, generated by Fe²⁺ oxidation (electron loss, astrocyte APP and CP) before binding with Tf and the influx into the neuron stroma, unconstrainedly floats in the extracellular space (neuropil) in the plaques vicinity. Probably, by effect of electrostatic forces (Coulomb force, electrostatic force, Coulomb interaction, $F = k \cdot Q1 \cdot Q2/d^2$, F = electrical force between two charged objects, $Q1$ and $Q2$ = the quantity of charge on object 1 and 2, d = distance of separation between two objects, k = Coulomb's law constant), the Fe³⁺ part, which does not bind with Tf (Tf and TfR1 are decreased in AD), is attracted to the A β 2 β 1 strand (A β , significantly elevated values in AD), and the primary electrostatic balanced position (N, N, O). These relatively labile connections (ion-dipole interaction), after the A β 1 approach, can transform into the six co-ordinate (dative) covalent bonds (N, N, N, N, O, O). Previous to this final bonding, under the electrostatic attraction by the approaching A β 1 monomer, Fe³⁺ is slightly elevated into the final electrostatic balanced position (precondition for covalent bonding). Before further analysis of Fe³⁺ binding with the imidazole ring, it is important to emphasize that TfR1 (transferin receptor1) is abundantly present on the luminal side of cerebral capillaries. Everything suggests that the Tf-TfR1 system is the crucial player in Fe³⁺ transmission through the blood brain barrier (BBB). Practically the same mechanism is crucial for Fe³⁺ entrance in the other body cells. Imidazole (molecular formula C₃H₄N₂) is actually

an anion (–) and therefore easily restitutes the mentioned attractive connection with Fe³⁺ which is a cation (+). The imidazole ring is very ionizable^{18,27}.

The pka value of the ring is roughly 7.0, so at the physiological pH (7.4) acidic and basic forms are present. The deprotonation of either N produces tautomers. N 1,3 have their lone pairs. Along with the N lone pair, Fe³⁺ electrostatic attraction is also influenced by a lone pair of the carbonyl oxygen peptide bonds between two neighbouring His residues. The analysis of the atom radii gives the obtained results: Fe²⁺ 0.76Å; Fe³⁺ 0.64Å; N 0.56Å. The values are approximately the same. The analysis of the presented facts casts doubt on further classic ionic bonding, and evidently indicates the secure development of the octahedral arrangement of ligands around the Fe³⁺ ion and six co-ordinate covalent bonds. It is evident that Fe³⁺ reduction occurs before the octahedral formation. In reality there are two parallel oxidation/reduction cycles. One cycle is related to MetS35, MetS35*, and MetSO, with the action of O₂*– and MsrA, and the other cycle is Fe³⁺, Fe²⁺, *OH, with the action of MetS35 and H₂O₂. Until the moment of complete formation of the complex ion and complete A β 1 rotation, Fe³⁺ reduction produces an infinite number of *OH molecules and harmful damages (Fig. 1-3)^{5,18,22}.

By applying the computational methodology, Ali-Torres J *et al.*²⁸) calculate the binding energy of Fe²⁺/Fe³⁺ with the His13-His14 sequence of A β , as well as His6 and Tyr10 (Tyr = tyrosine). Based on these investigations, they conclude that the optimal solution for both Fe³⁺ and Fe²⁺ is thermodynamically simultaneous binding with the His13-His14 complex and Tyr10. They also indicate that iron is the most abundant metal in senile plaques of obduction material of AD patients. The most stable complexes that contain the His13-His14 sequence and Tyr10 phenolate are pentacoordinated.

By connecting homology (HM) techniques with a quantum mechanics based approach (QM), in their following study, Ali-Torres J *et al.*²⁹) try to determine passable realistic three dimensional models for the Cu²⁺ - A β (1-16) complex with three His ligands around the central iron. They consider His6, His13, and His14, as well as several compounds containing O, as the fourth ligand (Asp1, Glu3, Asp7, Glu11, COAla2). In this study, Ali-Torres J *et al.*²⁹) in the presented scheme clearly explain the mentioned coordination sphere with Cu²⁺ and three His and Ala2 (Ala = alanine). One folded A β monomer is visible.

The next analysis about the binding between metal ions and His residues is presented by Kong X *et al.*³⁰). This group especially investigated the role of the His13-His14 sequence. By applying quantum chemical calculations they discovered that metal ions prefer three exactly defined positions (coordination sites) on the mentioned sequence, two on the imidazole ring nitrogen, and one on the peptide bond carbonyl oxygen. The strength of bonding was in the following order: K⁺ < Ca²⁺ < Zn²⁺ < Cu²⁺ < Fe³⁺ < Al³⁺. The strength of iron is clearly visible. The presented Fig. 1 in the paper clearly demonstrates the tridentate fashion of binding three ligands with the metal ion. The binding structure is composed of two nitrogens on imidazole rings and one oxygen on the carbonyl group. What is the type of this binding? The authors emphasize the possibility of a coordinated covalent (dative) bond with three included electron lone pairs, with a minimal possibility of ionic bonds (Fig. 2, 3).

Related to the mentioned investigations³⁰), our analysis

indicates the similarity with the primary threedentate structure of coordination. After the later binding of a metal ion with the incoming monomer, it is evident that there is the possibility of the formation of an octahedron. In the case of this arrangement, it can be seen that this is actually a strong ligand field. It is evident that splitting of d-orbitals is stronger with ligands which can, together with metal ions, generate the additional pi-bonding. These compounds are organic aromatic ligands, as is the imidazole ring in the case of the His13-His14 sequence. According to this fact, it is possible that hybridization can include two eg orbitals and some external orbitals (sp), depending on the real space arrangement, *i.e.* on the number of donor atoms. In the octahedral space arrangement of six donor atoms, the hybridization will be d^2sp^3 .

Similar to our reflections is the viewpoint of Nair NG *et al.*²²⁾ who also consider that the ligand space arrangement around the central metal ion is octahedral. They give great importance to histidine residues, especially to the imidazole nitrogen and carboxyl oxygen. On the other hand, we emphasize the importance of carbonyl oxygen as Kong X *et al.*³⁰⁾. The coordination with metal includes four nitrogen and two oxygen atoms. This strongly coincides with the number and character of our proposed ligands (4N and 2O) (*Fig. 2-6*)^{22,30)}.

The analysis of the Cu^{2+} and Zn^{2+} coordination chemistry in relation to $\text{A}\beta$ is presented in the studies by chemists Faller P and Hureau C^{31,32)}.

For better understanding of this type of bonding, it is necessary to consider in detail the meaning of complex ion. According to the ligand field theory (LFT), a complex ion is in fact a composite structure with a metal ion in its center (here Fe^{3+}), surrounded by several molecules or ions (ligands). Fe^{3+} does not have electrons in its 4s and 4p-orbitals, and five 3d-orbitals have one electron each. The d-orbitals have a different orientation in space (*Fig. 6*). In the case of more ligands, the hybridization (reorganisation) of 3d, s, and p Fe^{3+} ion orbitals creates an empty space which is able to accept the unshared pairs of electrons from ligands. The binding of Fe^{3+} and six ligands (after the $\text{A}\beta 1/\text{A}\beta 2$ aggregation) induces the sixdentate binding structure. Each ligand has in its outer energetic level one active electron pair. They are important for the formation of co-ordinate bonds with the central metal ion. It is important to emphasize that 3d-orbitals, five in the third shell, can accept 10 electrons: each of them can take two. Five d-electrons, which are not included in bonding, enter into three of the 3d-orbitals. The remaining 12 electrons enter into two 3d-orbitals, one 4s-orbital, and three 4-p orbitals (*Fig. 7-9*)^{33,34)}.

The actual question arises about the conditions of covalent bonding between ligands and Fe^{3+} . It is evident that in this process the crucial role lies in the reduction of their separation (d). It is also evident, according to Coulomb's law, that a decline of d value leads to the progressive rise in the attractive force F. This leads to a very unstable high-energy situation, energetically unfavorable. With the aim of preserving the energetic efficiency of the system, the approach stops (strong electrostatic influences) at an adequate optimal distance between involved factors. This distance is optimal for orbitals to overlap and the formation of coordinate (dative) covalent bonds. This type of bonding is practically the same as standard covalent bonding. The difference is only that in this type, the two bonding electrons are originated from one donor (ligand). The entrance of six lone pairs from ligands into the six empty hybridized

orbitals induces the formation of six coordinate covalent bonds accompanied with a favorable drop in the system energy.

It is important to emphasize other facts about the complex ion formation. During the well established $\text{A}\beta 1/\text{A}\beta 2$ parallel, congruent relation, there is a further slow approach between them. At the same time, there is a mild slow rotation (about 90 degree) of the two $\text{A}\beta 1$ imidazole rings contrary to the Z axis and toward the margin of the octahedron horizontal section. At the same time there is also a mild and slow rotation of the two imidazole rings that belong to the fixed $\text{A}\beta 2$ monomer. Rotation is contrary to the Z axis and also directed to the margin of the octahedron horizontal section. The complete octahedron structure is now visible. The rearrangement is the result of complex electrostatic force interactions. Below are some further explanations regarding this matter. The octahedral formation is actually the result of electrostatic interaction between the positive metal center and the negative ligand charge. In the event that the ligands are neutral polar molecules, the metal center reacts with their negative ends (ion-dipole attraction). Furthermore, ligands interact with one another also electrostatically (repulsion). The octahedron structure, with its lowest energy arrangement, causes minimal repulsive interactions between the ligands (VSEPR theory, *Fig. 5*)³⁴⁾.

Takeda T and Klimov DK^{35,36)} in their investigation about the $\text{A}\beta$ aggregation thermodynamics on the top of the preliminary formed protofilament, demonstrate that the aggregation is primarily linked to the one isolated incoming monomer. Interactions between monomers also occur, but evidently in the minimal rate. This finding supports our finding about the formation of the octahedral space structure of the metal complex with the Fe^{3+} ion in its center (the congruent contact between two parallel sequences: His13-His14/His13-His14) (*Fig. 2-4*).

The analysis of the $\text{A}\beta$ aggregation process evidently indicates that it is under the great influence of MOLD formation, as well as of the complex ion formation.

Aggregation, on the other hand, that is supporting the monomers approach, contributes to Fe^{3+} reduction and *OH generation. The role of the elevated iron concentrations on the aggregation process strengthening is especially emphasized by Hare D *et al.* (*Fig. 2,3*)^{5,19)}.

It is important to emphasize some facts connected with the aggregation process (*Fig. 2, 3*). The new $\text{A}\beta$ monomer attracted to the apical fixed monomer (electrostatic, hydrophilic and hydrophobic forces, H-bonds) arrives on the top and becomes fixed by the mentioned forces. This situation generates the possibility that the floating Fe^{3+} ion arrives on the adequate MBD and begins the fixation. The subsequent oblique nonparallel approach of the new $\text{A}\beta$ occurs, and continues the interaction of its MetS35 and $\text{A}\beta 2$ MBD (Fe^{3+}), Fe^{3+} reduction, $\text{A}\beta 1$ rotation, and finally the formation of the new complex ion. Aggregation continues and the protofilament grows⁵⁾.

The analysis of the central metal ion complex binding with ligands demonstrates that this event is not so simple. In the case when more than three ligands are present (in this case six), the explanation lies in the hybridization phenomenon of the outer empty two 3d, one 4s, and three 4p-orbitals (d^2sp^3), which leads to the creation of free space for the entrance of unpaired free electrons from ligands. Here are the six ligands (*Fig. 8,9*)^{32,37)}.

After the entrance in the region of possible attractive electrostatic interactions between Fe^{3+} ions and all six

A complex ion has a metal ion at its centre with a number of other molecules or ions surrounding it. These can be considered to be attached to the central ion by co-ordinate (dative) covalent bonds.

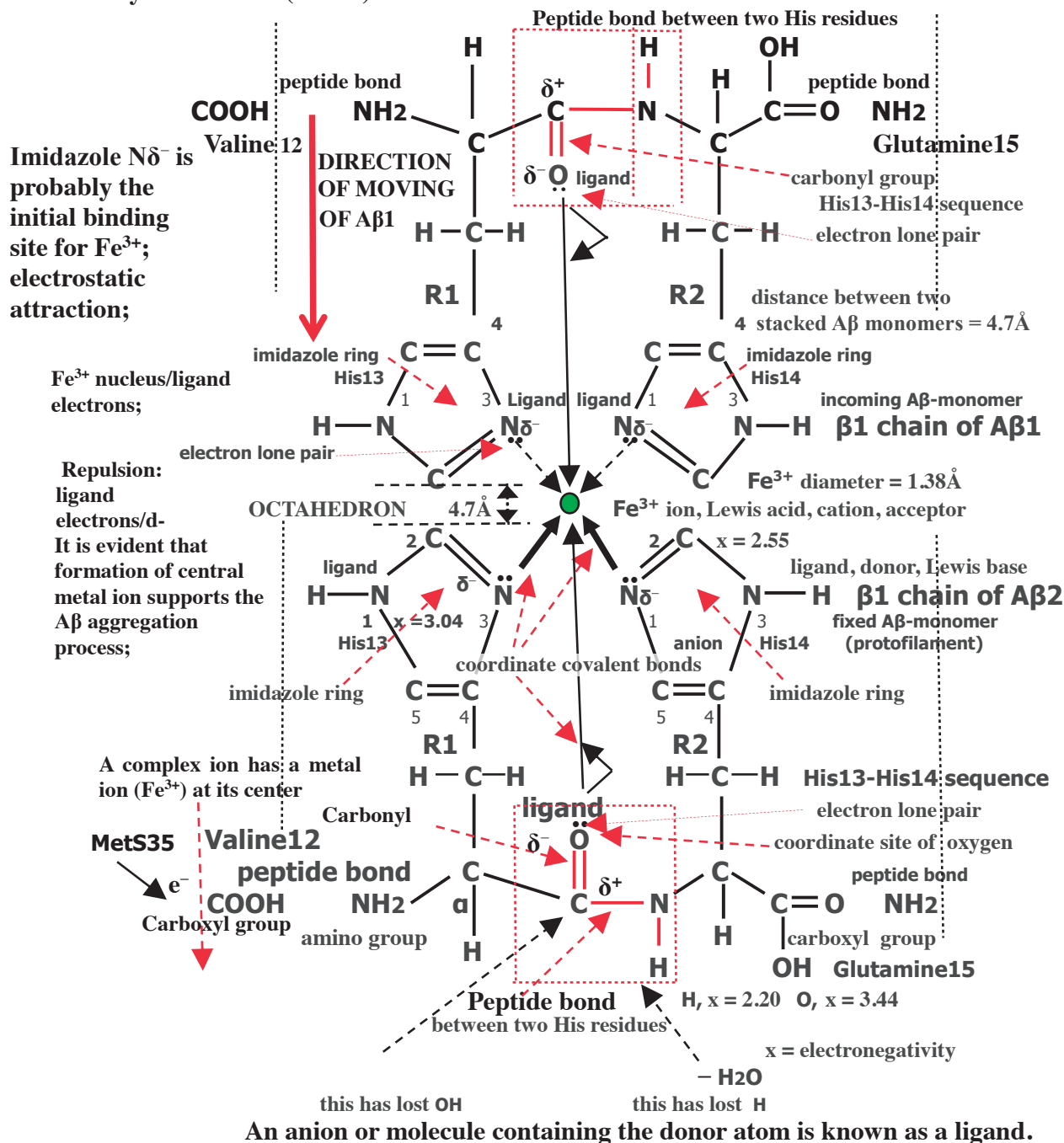


Fig. 4. Schematic presentation of the complex ion structure Me(His13-His14)2.

Coordinate covalent bonds, also known as coordinate links or semipolar bonds, are different from normal covalent bonds because both of the electrons that are shared by the bonded atoms originally come from the same atom. This contrasts with normal covalent bonds, in which each atom gives up one of the two electrons that form the shared electron pair; Me, metal; His, histidine, α -amino acid; glutamine 15 and valine 12, amino acids; MetS35, reduced methionine, amino acid, reduced form; Fe³⁺, ferric ion; A β , amyloid beta.

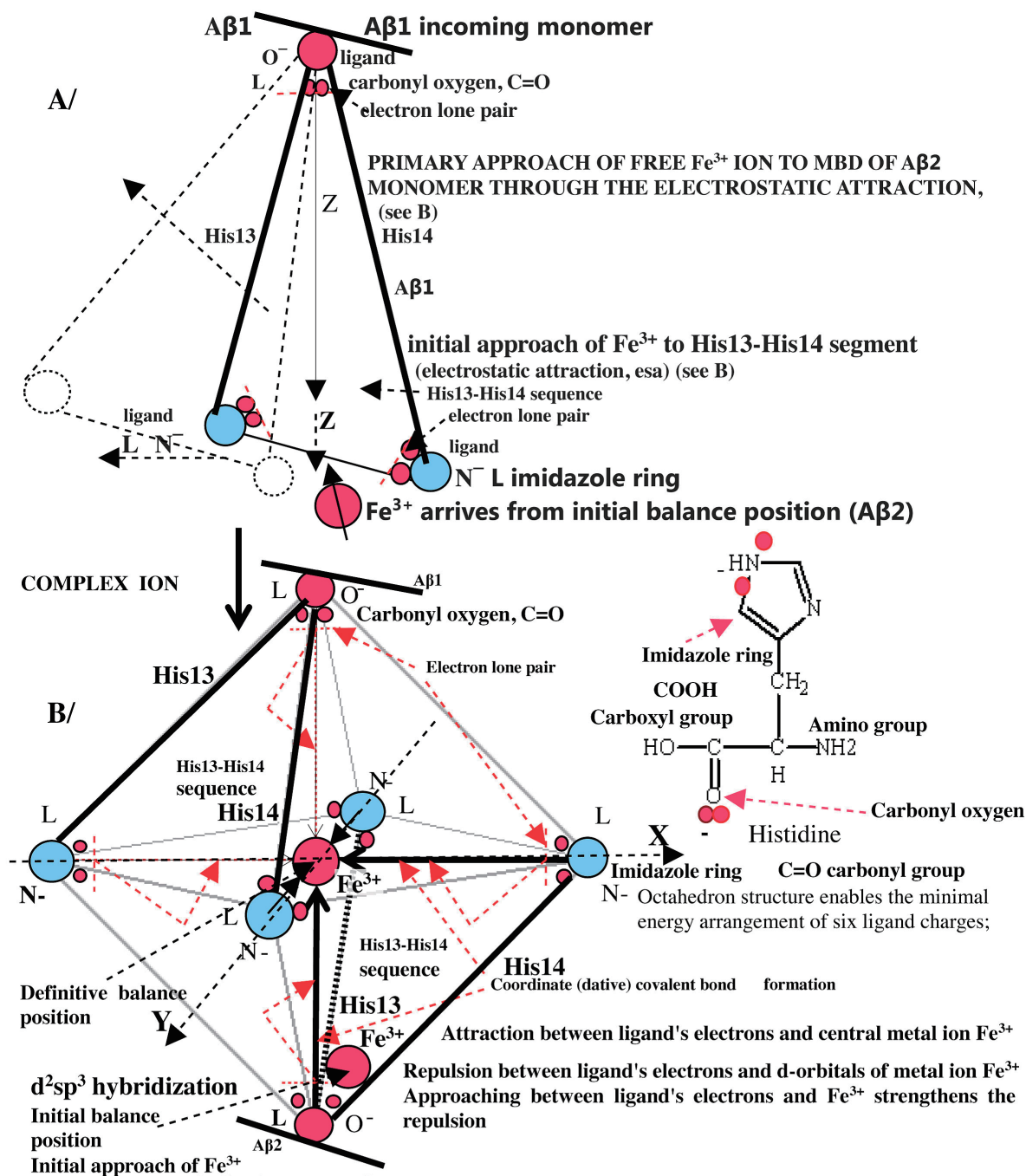


Fig. 5. Schematic presentation of the complex ion structure.

Section A/ : The upper part of the figure presents the approach of Fe^{3+} . Due to the approach of $\text{A}\beta 1$, through the effects of the electrostatic forces (described in the text), there is a slight rotation of His13-His14 in the direction of the dotted arrow (in the direction of the outer margin of the horizontal plane of the future octahedron), and the positioning of Fe^{3+} in the definite balance position. **Section B/ :** The definitive balance position of Fe^{3+} in the center of the formed octahedron. Fe^{3+} , from the initial balance position, by the effect of the electrostatic forces ($\text{A}\beta 1$ approach), rises into the definitive balance position. The octahedron is formed. It is clear that in the initial balance position, Fe^{3+} has arrived to the top of the $\text{A}\beta 2$ monomer slightly attracted by electrostatic forces (N, N, O). Octahedron, geometrical structure with eight triangular sides, twelve edges, and six vertices; His, histidine, amino acid, the component of $\text{A}\beta$; N, nitrogen; O, oxygen; imidazole, an organic compound, $\text{C}_3\text{N}_2\text{H}_4$; $\text{A}\beta$, amyloid beta; MBD, metal binding domain.

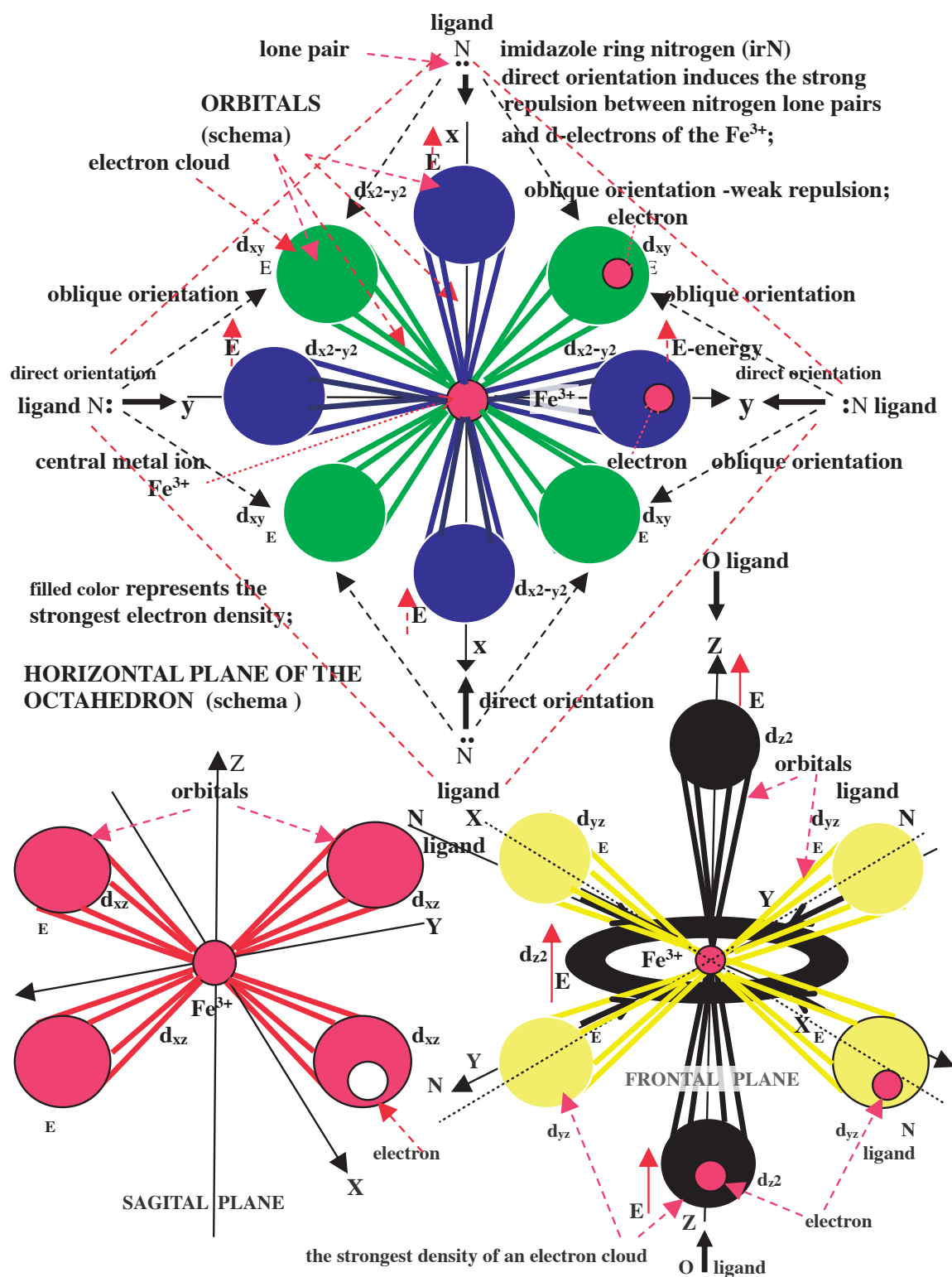


Fig. 6. Position of d_{z2} , d_{x2-y2} , d_{xz} , d_{xy} , and d_{yz} d-orbitals in the Cartesian coordinate system.

E, energy.

Primary approach of free Fe^{3+} ion to MBD (His6–His14) of the $\text{A}\beta 2$ monomer through electrostatic attraction (ligand electrons and Fe^{3+} nucleus, Coulomb law); Fe^{3+} ion has one empty 4s orbital, three empty 4p orbitals, and half filled five 3d orbitals.



Increased oblique, nonparallel approach of $\text{A}\beta 1$ to $\text{A}\beta 2$ (hydrophilic/hydrophobic forces, electrostatic forces) with the close encounter of MetS35 (reductant, $\text{A}\beta 1$, $\beta 2$ -strand) and MBD, ($\text{A}\beta 2$, $\beta 1$ -strand, with Fe^{3+} becoming closer to the reductant) causes electron "hop", Fe^{3+} reduction in Fe^{2+} , entry of Fe^{2+} into Fenton reaction and toxic $\cdot\text{OH}$ generation; $\text{Fe}^{2+} + \text{H}_2\text{O}_2 = \text{Fe}^{3+} + \cdot\text{OH} + ^-\text{OH}$. Everything points to the fact that quick reduction/oxidation with the presence of MetS35, MsrA (methionine sulfoxide reductase type A) and $\text{O}_2^{\cdot-}$ (superoxide radical anion) take place before the ion complex formation.



The increasing approach of Fe^{3+} and ligands to $\text{A}\beta 2$ (N,N,O) and $\text{A}\beta 1$ (N,N,O) results in energy growth of five degenerated (orbitals of equal energy) 3d orbitals of Fe^{3+} ion, they become excited orbitals. Due to different space directions of the five degenerated d orbitals, electrons in $d_{x^2-y^2}$ and d_{z^2} orbitals will be closer to the ligand electrons, and due to stronger repulsion they will have higher energy.



From the very beginning, due to further Fe^{3+} approach to the central position, the strong ligand field causes the splitting of five excited degenerated d-orbitals into two orbitals of higher energy e_g ($d_{x^2-y^2}$ and d_{z^2}) and three orbitals of lower energy t_{2g} (d_{xy} , d_{xz} , d_{yz}); five 3d orbital electrons are paired into three 3d orbitals, two 3d orbitals remain empty and they together with one 4s empty and three empty 4p orbitals enable Fe^{3+} bonding with six donor atoms from $\text{A}\beta 2$ and $\text{A}\beta 1$, causing the octahedral ionic complex onset; hybridisation (d^2sp^3) is essentially the consequence of the tendency to bond forming, to greater complex stability and the tendency to the complex total energy decline. Five paired electrons in three 3d orbitals do not participate in the bonding.



During the whole process of hybridisation (d^2sp^3) conditions have been made for the entrance of six pairs of lone electrons from ligands (4N and 2O) into the total of six hybridised empty orbitals.



The forming of six coordinate covalent bonds and the end of complete forming of the complex ion. There is no reduction any more because the space between MetS35 and MBD has grown to more than 19\AA . This increased space led to the end of the $\text{A}\beta 1$ complete rotation (hydrophobic forces, MOLD, H-bonds) and to the forming of the parallel congruent relation $\text{A}\beta 1/\text{A}\beta 2$ (aggregation completion).

Fig. 7. The sequence of the complex ion $\text{Fe}(\text{His13-His14})_2$ formation and basic pathophysiological events crucial for the development and course of Alzheimer's disease.

Fe^{3+} , ferric ion, redox inactive iron, non-toxic; Fe^{2+} , ferrous ion, redox active iron, toxic; $\cdot\text{OH}$, toxic, aggressive hydroxyl radical; ^-OH , non-toxic hydroxyl ion, reduction, electron gain; oxidation, electron loss; MetS35, reduced methionine, amino acid, the component of $\text{A}\beta$ monomer; MsrA, methionine sulfoxide reductase type A; MBD, metal binding domain, a sequence (His6-His14) on $\text{A}\beta$ $\beta 1$ strand; $\text{A}\beta$, amyloid beta; His, histidine; MOLD, methylglyoxal lysine dimer.

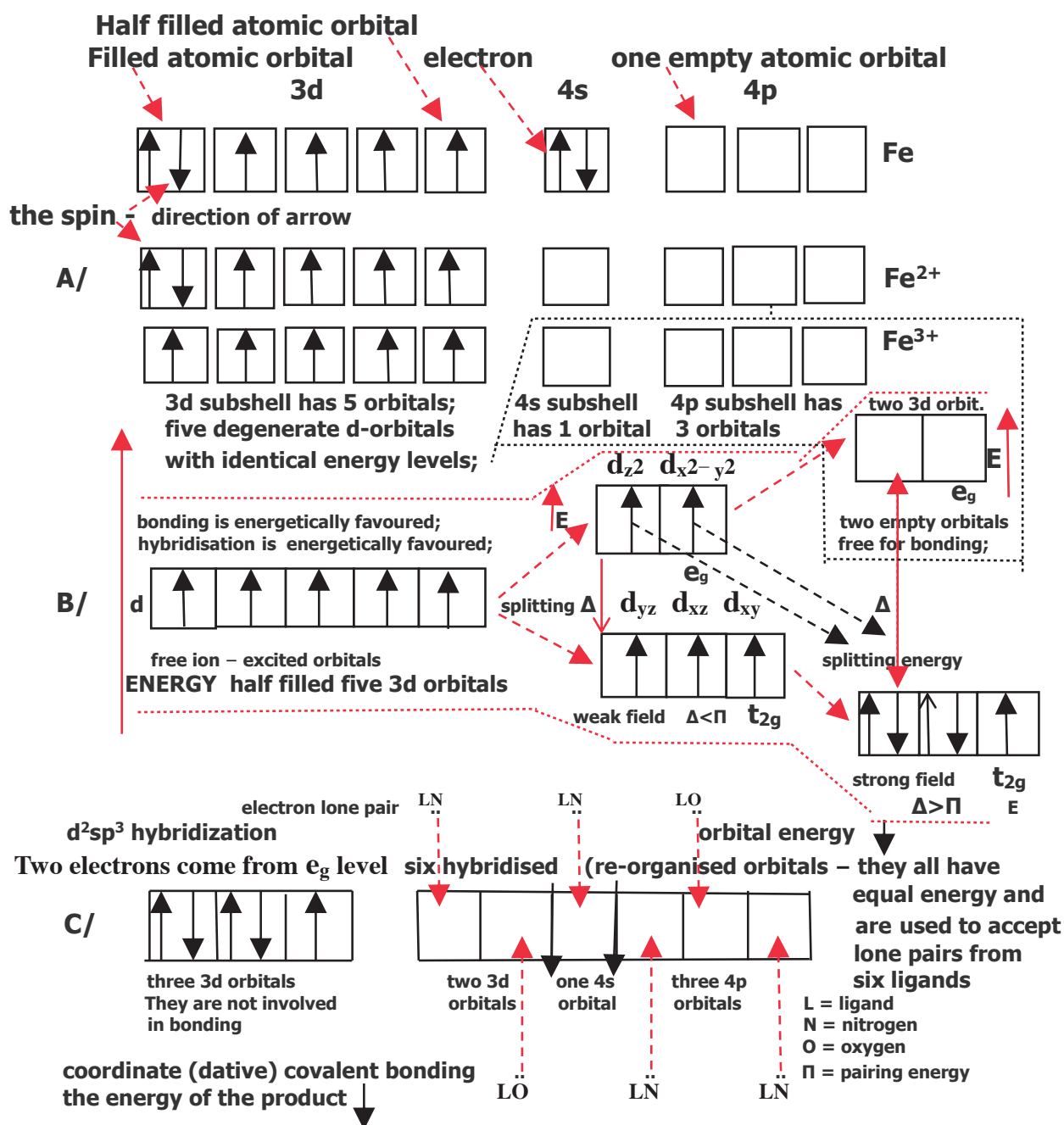


Fig. 8. Electronic configuration of iron atom (Fe) and its ions (Fe²⁺, ferrous ion) and (Fe³⁺, ferric ion) in the highest filled quantum levels.

Survey of electronic configuration of iron (Fe) and its ions. For Fe it is: 1s² 2s² 2p⁶ 3s² 3p⁶ 4s² 3d⁶; for Fe²⁺ is: 1s² 2s² 2p⁶ 3s² 3p⁶ 3d⁶; for Fe³⁺ is: 1s² 2s² 2p⁶ 3s² 3p⁶ 3d⁵. In the first shell (n = 1) is one 1s orbital which can hold 2 electrons; in the second shell (n = 2) are 2 s orbitals (total 2 electrons) and 2p orbitals (total 6 electrons), in the second shell there are 8 electrons; in the third shell (n = 3) there is one 3s orbital (2 electrons), 3p orbitals (total 6 electrons), 3d orbitals are composed of 5 d orbitals and one can hold 2 electrons, these 5 d orbitals can hold 10 electrons. Fe³⁺ in the third shell has 5 electrons in 5 d orbitals (in every orbital there is 1 electron-valence electron); every d orbital can hold 2 electrons. It is important to know that shells and orbitals are not the same thing. It is evident that 3d orbitals can also accept one electron which has a reductive function; L, ligand; atom has an infinite number of orbitals, it has a finite number of filled orbitals and only one valence orbital; lower energy, triple-degenerate set (the t_{2g} orbitals); higher energy, double-degenerate set (the e_g orbitals).

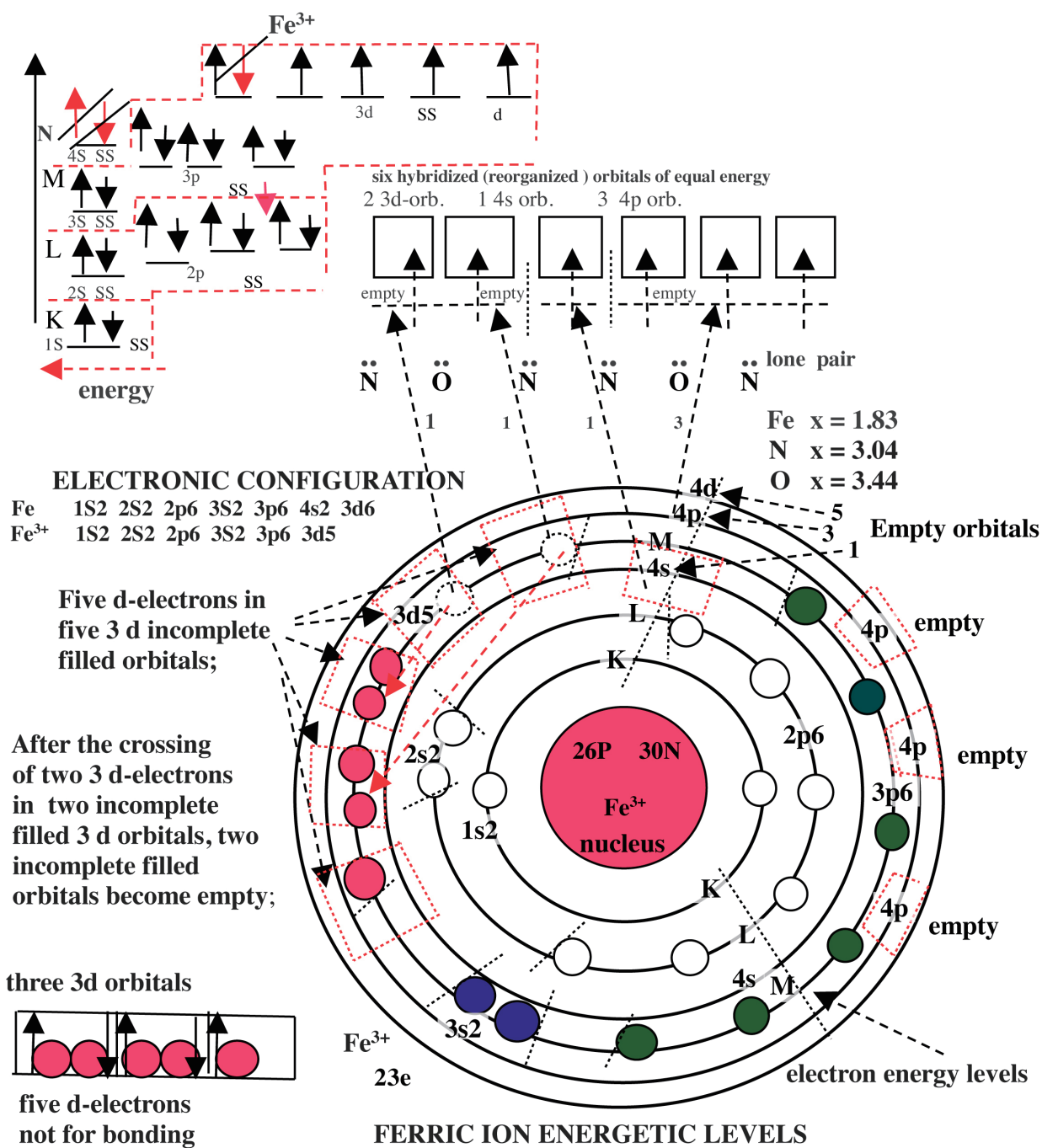


Fig. 9. Electronic structure of ferric ion (Fe^{3+}).

K, first shell, has one subshell 1s², 2 e⁻; L, second shell, has two subshells, 2s, 2 e⁻, 2p, 6 e⁻; M, third shell, has three subshells, 3s, 2 e⁻; 3p, 6 e⁻; and 3d, 5 e⁻; ss, subshell; O, oxygen, 2e⁻, one lone pair; N, nitrogen, 2e⁻, one lone pair; x, electronegativity; eel, electron energy level; before hybridization and Fe³⁺ bonding with ligands five d-electrons were in five 3d incomplete filled 3d orbitals; 4s one and 4p three orbitals were also empty; orb., orbital.

ligands, the Fe^{3+} ion, previously located near the A β 2 His13-His14 sequence, is subsequently attracted by Coulomb's forces closer to the incoming complex A β 1 and its His13-His14 sequence. As it is presented earlier, the prerequisite for the future binding of metal ions and ligands into a complex ion is the creation of six empty Fe^{3+} outer orbitals capable of the acceptance of six lone pairs. This was the precondition for the formation of six coordinate covalent bonds. During these events, the formation of five excited d-orbitals is necessary (the reason for this formation is the induced rise in energy of primary d-orbitals), and related to their spatial orientation, their consequent splitting on two orbitals with higher energy (e_g - d_{z^2} , $d_{x^2-y^2}$) and three with lower energy (t_{2g} - d_{xy} , d_{xz} , d_{yz}) (Fig. 2, 6, 8, 9)^{33,34}.

Coordinate covalent bonds are types of polar bonds according to the difference in the electronegativity between Fe^{3+} and ligands (Fe, $x = 1.83$; N, $x = 3.04$; O, $x = 3.44$). It is evident that the electron cloud is attracted to the ligand side of the bond. The origin of electrons in the bond is one atom^{33,36}.

At the beginning, the Fe^{3+} ion that is attracted by the simultaneous effects of the three negative charges of the included ligands (A β 2 - N, N, O) is moving firstly towards the initial balance position on the A β 2 monomer. Based on the approach of A β 1 and the rise of a new attraction, Fe^{3+} moves into the definitive balance position (the central position of the formed complex ion). Fe^{3+} d-electrons become exposed to the rise of repulsion between them and ligand electrons. As it was previously presented, the difference in the repulsive strength results in d-orbital splitting into two different groups. The energy of splitting is higher when the ligand field is stronger. And the ligand field is stronger in relation to the higher vicinity between the electrons of the two systems. If the energy of splitting (Δ) is higher than the energy of pairing (Π), five d-electrons will be paired in three lower energy orbitals (t_{2g}). Two orbitals of higher energy (e_g) remain free for binding with ligands. This leads to the hybridization d^2sp^3 with the octahedral space structure of the formed complex ion (Fig. 5-8)^{33,34}.

Fe^{3+} , which does not have a structure of noble gases, *i.e.* it has completely empty s, p, and partially empty 3d-orbitals, aspires to complete these orbitals by binding other ions or molecules that have free lone pairs. After this binding, the electronic configuration corresponds to the electronic configuration of noble gases, and energetic stability is high (octet rule). Every atom has the natural tendency for the formation of favoured chemical bonds and, in this way, for high energetic stability (Fig. 8, 9)³³.

The formed coordinate covalent bond, according to the different electronegativity (x) between Fe^{3+} and the ligands, has a positive (+) and partially negative (δ^-) end. Fe^{3+} presents the positive end and N and O are partially negative. This type of bond is the polar bond. On the other hand, it is important to mention that an electron *per se* is also dipole (it has an electric dipole moment EDM). According to the well known interaction between positive ions and negative subatomic particles, it is clear that the positive Fe^{3+} charge can attract the electron³³.

The explanation of the presented interaction between the metal ion and histidine residues is given by the Crystal Field Theory. This theory considers that the ligands binding to the metal in the complex ion is primarily an electrostatic phenomenon, related to the covalence. In fact, here are two types of electrostatic interactions. The first one is the

attraction between the positive metal charge and negative charge of ligand electron lone pairs. The second type of interaction is the originated repulsion between ligand lone pairs and 3d-orbital electrons of metal. This theory explains the specific characteristics of the transition metal complexes but does not try to explain the bonding process. Later, this theory was excellently complemented by the Molecular Orbital Theory with the formation of the more perfect Ligand Field Theory (LFT), which elucidated the chemical bonding in the mentioned complexes³³.

The hybridization (re-organization) of orbitals is naturally favored because hybridized orbitals have lower energy in relation to their original, unhybridized copies. The results are more stable compounds after hybridization. Major parts of these hybridized orbitals, or frontal lobes, overlap better than those of unhybridized orbitals. The result is better bonding³³.

It is necessary to direct attention to the consideration of some researchers who are involved in the problem matter of Fe^{3+} binding with A β . All these researchers give importance to the A β His13-His14 sequence, to the role of redox-active metals, destructive effects of reactive oxygen species (ROS), and oxidative stress. The exploration of the complex intra and intermolecular events in the senile plaque demands further intensive action³⁷⁻⁴².

The analysis of the presented considerations and experimental results undoubtedly demonstrates the great importance of iron ions in the pathology and pathophysiology of AD. Significant is the importance of Fe^{3+} reduction into Fe^{2+} with consequent Fenton reaction and destructive $\cdot\text{OH}$ generation. A number of investigators point out the N-terminal part of β 1 strand as the crucial place for metal binding (first 16 residues). According to their results, the most important region is the His13-His14 sequence. The position of the central metal ion is located in the center of the octahedral structure. The crucial events during this binding lie in the complex intermolecular interactions that include molecular orbital hybridization type d^2sp^3 and the formation of coordinate covalent bonds between the central metal ion and ligands. Although knowledge about these processes grows every day, there is the necessity for further intensive investigations about this problem.

Why is it so important to exactly determine the binding site of Fe^{3+} on A β ? The progress in AD chelation therapy can give the explanation. Chelates (a chemical compounds composed of a metal ion and a chelating agent), especially from the iron group, are complex compounds which can be connected with nanoparticles, and can pass through the BBB and dissolve amyloid plaques. Budimir A⁴³) in her study presents the effects of Desferrioxamine B (DFO, Desferal[®]) and a number of 8-hydroxyquinoline analogs in the therapy of AD. Among them, they analysed clioquinol (PBT1), and the more effective and practically harmless PBT2. Liu G *et al.*⁴⁴) in their study present the efficiency of the chelator-nanoparticle system complexed with iron, also used in the therapy of AD. In their other study,⁴⁵) present the favourable effects of DFO, Deferiprone, Deferasirox, and clioquinol. Chelation therapy needs yet more intensive analysis and investigations⁴⁶). Muralidhar LH *et al.*²⁵) in their study also present the positive effects of chelation therapy of AD.

Although this study is primarily concerned with the pathophysiology of AD and a short review of chelation therapy, its authors believe that it was necessary to present some facts about the other therapeutic media. The blockade of MOLD

generation and its disintegration is possible by alagebrium (ALT-711; DMTB [N-phenacyl-4,5-dimethyl bromide], the breaker of already formed crosslinked compounds). The therapy also includes: aminoguanidine (CH_6N_4 , pimegidine – suppressor of crosslinking, nitric oxide synthase inhibitor); DPTC (4,5-dimethyl-3-phenacylthiazolium chloride—a crosslinked compound breaker). *Ginkgo biloba* has a strong neuroprotective, anti-apoptotic and anti-oxidative capacity. Anti-oxidative vitamins are also used in AD therapy (vitamin C, α -tocopherol, thiamine, pyridoxamine). Recently, the actual medicamentous AD therapy consists of two groups of medicaments. The first group consists of cholinesterase blockers: Aricept (donepezil hydrochloride), Axelon (rivastigmine), and Reminyl (galantamine hydrochloride). The second group includes N-methyl-D-aspartate (NMDA) receptor (NMDAR) antagonists, as well as Ebixa (memantine) ^{17,47}.

Conclusion

AD is a serious, chronic, progressive neurodegenerative disease with polygenetic ethiology. The exact cause is still unknown. All recent investigations point out the crucial role of oxidative stress in the origin of this disease, as well as in

its future development and patophysiological and pathologic events. Especially significant is the role of iron, with reference to its ions, Fe^{3+} and Fe^{2+} . Connected with these ions, the Fenton reaction, accompanied with the generation of extremely aggressive and toxic $\cdot\text{OH}$, is probably crucial among these patophysiological events. The Fe^{3+} ion, attracted by electrostatic forces, arrives very early on the $\beta 1$ strand of the newly formed and in the interstitium released $\text{A}\beta$ monomer; in this position it is fixed and reduced by MetS35 in Fe^{2+} , and incorporated into the Fenton reaction. The essential question, which this study attempts to answer is the exact definition of the Fe^{3+} binding place and the method of this binding. All investigations indicate the complexity of this process which includes a series of intermolecular interactions, including Fe^{3+} atomic orbital hybridization (d^2sp^3) and its binding with neighbouring octahedrally arranged ligands located on the two parallel and congruently situated $\text{A}\beta$ sequences. These complex events demand further investigations.

Conflict of interest

The authors claim no conflict of interest in this study.

References

- Smith DG, Cappai R, Bamham KJ. The redox chemistry of the Alzheimer's disease amyloid β peptide. *Biochim Biophys Acta*. 2007; 1768: 1976-1990.
- Everett J, Cespedes E, Shelford LR, et al. Evidence of redox-active iron formation following aggregation of ferrihydrite and the Alzheimer's disease peptide β -amyloid. *Inorg Chem*. 2014; 53: 2803-2809.
- Everett J, Cespedes E, Shelford LR, et al. Ferrous iron formation following the coaggregation of ferric iron and the Alzheimer's disease peptide β -amyloid (1-42). *J R Soc Interface*. 2014; 11: 20140165.
- Huang WJ, Zhang XIA, Chen WW. Role of oxidative stress in Alzheimer's disease. *Biomed Rep*. 2016; 4: 519-522.
- Barić N. Role of advanced glycation end products (AGEs) on the reactive oxygen species (ROS) generation in Alzheimer's disease amyloid plaque. *Glycative Stress Res*. 2015; 2: 140-155.
- Saharan S, Mandal PK. The emerging role of glutathione in Alzheimer's disease. *J Alzheimers Dis*. 2014; 40: 519-529.
- Mandal PK, Saharan S, Tripathi M, et al. Brain glutathione levels—a novel biomarker for mild cognitive impairment and Alzheimer's disease. *Biol Psychiatry*. 2015; 78: 702-710.
- Murakami K, Murata N, Noda Y, et al. SOD1 (copper/zinc superoxide dismutase) deficiency drives amyloid β protein oligomerization and memory loss in mouse model of Alzheimer's disease. *J Biol Chem*. 2011; 286: 44557-44568.
- Angeloni C, Zamboni L, Hrelia S. Role of methylglyoxal in Alzheimer's disease. *Biomed Res Int*. 2014; 2014: 238485.
- Maynard CJ, Bush AI, Masters CL, et al. Metals and amyloid- β in Alzheimer's disease. *Int J Exp Pathol*. 2005; 86: 147-159.
- Ott S, Dziadulewicz N, Crowther DC. Iron is a specific cofactor for distinct oxidation- and aggregation- dependent $\text{A}\beta$ toxicity mechanisms in *Drosophila* model. *Dis Model Mech*. 2015; 8: 657-667.
- Li Na Zhao, Yuguang Mu, Lock Yue Chew. Heme prevents amyloid betapeptide aggregation through hydrophobic interaction based on molecular dynamics simulation. *Phys Chem Chem Phys*. 2013; 15: 14098-14106.
- Jiang D, Li X, Williams R, et al. Ternary complexes of iron, amyloid- β and nitrilotriacetic acid. *Biochemistry*. 2009; 48: 7939-7947.
- Streltsov VA, Titmuss SJ, Epa VC, et al. The structure of the amyloid- β peptide high-affinity copper II binding site in Alzheimer disease. *Biophys J*. 2008; 95: 3447-3456.
- Gaeta A, Hider RC. The crucial role of metal ions in neurodegeneration: the basis for a promising therapeutic strategy. *BJP*. 2005; 146: 1041-1059.
- Collingwood JF, Chong RKK, Kasama T. Three-dimensional tomographic imaging and characterization of iron compounds within Alzheimer's plaque core material. *Journal of Alzheimer's disease*. 2008; 14: 235-245.
- Barić N. Role of advanced glycation end products in Alzheimer's disease. *Glycative Stress Res*. 2014; 1: 68-83.
- Oshiro S, Marioka MS, Kikuchi M. Dysregulation of iron metabolism in Alzheimer's disease, Parkinson's disease, and amyotrophic lateral sclerosis. *Adv Pharmacol Sci*. 2011; 2011: 378278.

- 19) Hare D, Ayton S, Bush A, et al. A delicate balance: Iron metabolism and diseases of the brain. *Front Aging Neurosci.* 2013; 5: 34.
- 20) Schöneich C. Methionine oxidation by reactive oxygen species: Reaction mechanisms and relevance to Alzheimer's disease. *Biochim Biophys Acta.* 2005; 1703: 111-119.
- 21) Page CC, Moser CC, Chen X, et al. Natural engineering principles of electron tunneling in biological oxidation-reduction. *Nature.* 1999; 402: 47-52.
- 22) Nair NG, Perry G, Smith MA, et al. NMR studies of zinc, copper, and iron binding to histidine, the principal metal ion complexing site of amyloid-beta peptide. *J Alzheimers Dis.* 2010; 20: 57-66.
- 23) Minicozzi V, Stellato F, Comai M, et al. Identifying the minimal copper- and zinc-binding site sequence in amyloid-beta peptides. *J Biol Chem.* 2008; 283: 10784-10792.
- 24) Hane F, Leonenko Z. Effect of metals on kinetic pathways of amyloid- β aggregation. *Biomolecules.* 2014; 4: 101-116.
- 25) Hedge ML, Bharathi P, Suram Anitha, et al. Challenges associated with metal chelation therapy in Alzheimer's disease. *Journal of Alzheimer's Disease.* 2009; 17: 457-468.
- 26) Istrate AN, Kozin SA, Zhokhov SS, et al. Interplay of histidine residues of the Alzheimer's disease A β peptide governs its Zn-induced oligomerization. *Sci Rep.* 2016; 6: 21734.
- 27) Peters DG, Connor JR, Meadowcroft MD. The relationship between iron dyshomeostasis and amyloidogenesis in Alzheimer's disease: two sides of the same coin. *Neurobiol Dis.* 2015; 81: 49-65.
- 28) Ali-Torres J, Rodriguez-Santiago L, Sodupe, M, et al. Structures and stabilities of Fe^{2+/3+} complexes relevant to Alzheimer's disease: An Ab initio study. *J Phys Chem A.* 2011; 115: 12523-12530.
- 29) Ali-Torres J, Maréchal JD, Rodrigues-Santiago L, et al. Three dimensional models of Cu²⁺-A β (1-16) complexes from computational approaches. *J Am Chem Soc.* 2011; 133: 15008-15014.
- 30) Kong X, Zhao Z, Lei X, et al. On the interaction of metal ions with the His13-His14 sequence relevant to Alzheimer's disease. *J Phys Chem A.* 2015; 119: 3528-3534.
- 31) Faller P, Hureau C. Bioinorganic chemistry of copper and zinc ions coordinated to amyloid -beta peptide. *Dalton Trans.* 2009; 21: 1080-1094.
- 32) Faller P. Copper and zinc binding to amyloid-beta: Coordination, dynamics, aggregation, reactivity and metal-ion transfer. *ChemBiochem.* 2009; 10: 2837-2845.
- 33) Filipović I, Lipanović S. Poglavlje 6.13. Kompleksni spojevi, pg.306-352, in *Opća i anorganska kemija-I dio-opća kemija, VII izdanje, Školska knjiga, Zagreb, 1988.*
- 34) Sathyanarayana DN. Crystal field and ligand field theories. In: Sathyanarayana DN, Sathyanarayana DN, ed. *Electronic absorption spectroscopy and related techniques.* Universities Press (India), Hyderabad (India): 2001, pp.98-136.
- 35) Takeda T, Klimov DK. Replica exchange simulations of the thermodynamics of A β fibril growth. *Biophysical Journal.* 2009; 96: 442-452.
- 36) Nakamura M., Shishido N, Nunomura A, et al. Three histidine residues of amyloid-beta peptide control the redox activity of copper and iron. *Biochemistry.* 2007; 46: 12737-12743
- 37) Filipović I, Lipanović S. Poglavlje 6.3. Kovalentna veza, pg 196-201, in *Opća i anorganska kemija-I dio-opća kemija, VII izdanje, Školska knjiga, Zagreb, 1988.*
- 38) Epa VC. Structural and computational studies of interactions of metals with amyloid beta. DOI:10.5772/32786.2012; 15-36
- 39) Raffa DF, Gómez-Balderas R, Brunelle P, et al. Ab initio model studies of copper binding to peptides containing a His-His sequence: Relevance to the beta-amyloid peptide of Alzheimer's disease. *J Biol Inorg Chem.* 2005; 10: 887-902
- 40) Raffa DF, Rickard GA, Rauk A. Ab initio modelling of the structure and redox behaviour of copper (I) bound to a His-His model peptide:relevance to the disease. *J Biol Inorg Chem.* 2007; 12: 147-64.
- 41) Miura T, Suzuki K, Kohata N, et al. Metal binding modes of Alzheimer's amyloid β -peptide in insoluble aggregates and soluble complexes. *Biochemistry.* 2000; 39: 7024-7031.
- 42) Miura T, Suzuki K, Takeuchi H, et al. Binding of iron(III) to the single tyrosine residue of an amyloid - β peptide probed by Raman Spectroscopy. *Journal of Molecular Structure.* 2001; 598: 79-84.
- 43) Budimir A. Metal ions, Alzheimer's disease and chelation therapy. *Acta Pharm.* 2011; 61: 1-14.
- 44) Liu G, Men P, Harris PL. Nanoparticles iron chelators: A new therapeutic approach in Alzheimer disease and other neurologic disorders associated with trace metal imbalance . *Neurosci Lett.* 2006; 406: 189-193.
- 45) Liu G, Men P, Perry G. Nanoparticle and iron chelators as a potential novel Alzheimer therapy. *Methods Mol Biol.* 2010; 610: 123-144.
- 46) Rottkamp CA, Raina AK, Zhu X. Redox-active iron mediates amyloid-beta toxicity. *Free Radic Biol Med.* 2001; 30: 447-450.
- 47) Barić N. Interaction of methylglyoxal lysine dimer (MOLD) and hydrophobic/hydrophylic forces in the patophysiology of Alzheimer's disease. *Glycative Stress Res.* 2017; 4: 1-15.